Froissaron and Maximal Odderon with spin-flip in pp and $\bar{p}p$ high energy elastic scattering

N. Bence,

Uzhgorod National University, 88017 Universitetska street, 14, Uzhgorod, e-mail: bencenorbert007@gmail.com

A. Lengyel, Z. Tarics,

Institute of Electron Physics of NAS of Ukraine, 88017 Universytetska street. 21, Uzhgorod e-mails: alexanderlengyel39@gmail.com; tarics1@rambler.ru

E. Martynov, G. Tersimonov,

Bogolyubov Institute for Theoretical Physics of NAS of Ukraine, 03143, Metrologicheskaja st. 14b, Kiev-143, Ukraine. e-mails: martynov@bitp.kiev.ua; tersimonov@bitp.kiev.ua (Dated: March 14, 2022)

We assume that the scattering amplitude is represented by Froissaron, Maximal Odderon as well as by standard Regge poles. From the fit to the data of pp and $\bar{p}p$ scattering at high energy and not too large momentum transfers we found that this model taking into account the spin is available to describe not only the differential, total cross section and ρ , but also the existing experimental data on polarization.

INTRODUCTION

The polarization data available at present for protonproton scattering at relatively high energies are compatible with s-channel helicity conservation [1–3] and show that the polarization contribution decreases with increasing energy as it is expected in terms of Regge pole exchanges. The data are insufficiently precise to provide unambiguous conclusion at the higher energy, although a contribution from the helicity-flip amplitude cannot be excluded [2, 4–6]. The existing polarized experiments [7–10] at energy lower than LHC allow one to study spin properties of proton-pomeron vertex at intermediate energies while conclusions about spin properties of amplitudes at high t are derived as rule from model extrapolations.

The main conclusion was made that pomeron exchange is expected to produce the observed small spin effects.

Despite of a long time interest to spin effects physics in hadron interaction the available data set is not rich in a soft kinematic region. Firstly, the main part of experiments was performed for meson-nucleon and electron-proton interactions. Secondly, these measurements were made at low and middle energies. Nevertheless, the available data stimulate permanently the theoretical and phenomenological studies of spin phenomena in the regions of soft and hard kinematic were different approaches (non-perturbative approaches from early [11] to relatively later and recent [6, 12–15], and perturbative QCD) are exploring [16].

Unfortunately, there are almost absent the experimental data on spin observable quantities at highest energies which would to give additional information about properties of helicity amplitudes. As we known only the data at

FNAL energies [7–9] and the relatively recent data from RHIC [10] (however, at very small t, in Coulomb-nuclear interference region) are available.

However, now thanks to series of CERN TOTEM proton-proton experiments [17–20] we possess the long-awaited complete set of the precise data for testing various models over a wide range of energy and momentum transfer. Proton-proton (antiproton) scattering is the unique possibility to investigate crossing-odd contribution and its spin-flip properties.

The Froissaron and Maximal Odderon model (FMO model) [21–24] has recently successfully described such an extended set of experimental data. Therefore, the idea to extend the application of this model to consider some of the spin effects, for instance, polarization data of pp scattering at relatively high energy naturally arises. This task has been around for a long time, although attempts to solve it are rarely undertaken, as we noted above, due to lack of sufficiently precise data at highest energies.

The main interest of the present paper is concentrated, after new measurements at the LHC, on the questions "Do Froissaron and Maximal Odderon flip spin?" and "How big are crossing-even and crossing-odd spin-flip amplitudes comparing with the corresponding spin-non-flip-amplitudes? ". We examine the issue in the framework of the Froissaron and Maximal Odderon model. In Froissaron and Maximal Odderon approach we restrict ourselves to taking into account the contribution of two amplitudes: spin-non-flip and the single spin-flip one.

The paper is organized as follows. In the next section the main formulas and general discussion of the problems are presented. In Section II A we describe the Simplified FMO amplitude. In the Section II B we discuss the original FMO model with spin-flip amplitudes. The results

of comparison of both the models with data at $\sqrt{s} > 19$ GeV and at intermediate t is given in the Section III.

To avoid the inevitable increase in the number of parameters, we use similarly to many authors [1–6, 12, 14, 15] some simplified assumptions about spin-non-flip and spin-flip amplitudes and their relationship.

I. DEFINITIONS AND THE FMO APPROACH

A. Helicity amplitudes, observables

Generally the proton-proton and antiproton-proton scattering amplitude reads as

$$A_{\bar{p}p}^{pp}(s,t) = A^{(+)}(s,t) \pm A^{(-)}(s,t). \tag{1}$$

In this model we used the following normalization of the averaged in spin physical amplitudes

$$\sigma_t(s) = \frac{1}{\sqrt{s(s - 4m^2)}} \text{Im} A(s, 0),$$

$$\frac{d\sigma_{el}}{dt} = \frac{1}{64\pi k s(s - 4m^2)} |A(s, t)|^2$$
(2)

where $k=0.3893797~\text{mb}\cdot\text{GeV}^2$. With this normalization the amplitudes have dimension $\text{mb}\cdot\text{GeV}^2$ and all the couplings are given in millibarns.

Accounting the spin degrees of freedom in nucleonnucleon elastic scattering stills as a not well defined and quite complicated procedure. There are no the strict and consequent methods to construct the 5 independent helicity amplitudes for elastic nucleon-nucleon interaction:

$$\begin{split} &\Phi_{1}(s,t) = < + + |\mathcal{T}| + + >, \\ &\Phi_{2}(s,t) = < + + |\mathcal{T}| - - >, \\ &\Phi_{3}(s,t) = < + - |\mathcal{T}| + - >, \\ &\Phi_{4}(s,t) = < + - |\mathcal{T}| - + >, \\ &\Phi_{5}(s,t) = < + + |\mathcal{T}| + - >. \end{split} \tag{3}$$

Only various phenomenological models for this amplitudes have been constructed and analyzing. Each of these amplitudes has crossing-even and crossing-odd components $\Phi_i(s,t)$, i=1,2,...,5

$$\Phi_{\bar{p}p}^{pp}(s,t) = \Phi^{(+)}(s,t) \pm \Phi^{(-)}(s,t). \tag{4}$$

For the spin-averaged initial protons (antiprotons) the following equations for the total and differential cross sections and polarization are used

$$\sigma_{tot} = \frac{1}{\sqrt{s(s - 4m^2)}} \operatorname{Im} \left(\Phi_1 + \Phi_3\right), \tag{5}$$

$$\frac{d\sigma_{el}}{dt} = \frac{1}{16\pi ks(s - 4m^2)} \times (|\Phi_1|^2 + |\Phi_2|^2 + |\Phi_3|^2 + |\Phi_4|^2 + 4|\Phi_5|^2),$$
(6)

$$P(t) = -2 \frac{\operatorname{Im}[(\Phi_1 + \Phi_2 + \Phi_3 - \Phi_4)\Phi_5^*]}{|\Phi_1|^2 + |\Phi_2|^2 + |\Phi_3|^2 + |\Phi_4|^2 + 4|\Phi_5|^2}.$$
 (7)

Therefore in what follows we consider the case with $\Phi_2 = \Phi_3 = \Phi_4 = 0$, assuming in accordance with a common opinion that other spin amplitudes are small at high energies [1, 2, 4, 6, 12, 14, 15].

B. FMO approach

Let's comment shortly the Foissaron and Maximal Odderon approach to elastic proton-proton (antiproton) elastic scattering. Two realizations of it are explored in the paper.

Historically it was formulated in the [21] and applied [22–24] in description of high energy data on pp and $\bar{p}p$ scattering including the newest TOTEM data at 13 TeV.

The maximal growth of the even-under-crossing amplitude $A^{(+)}$ allowed by unitarity is

$$A^{(+)}(s, t = 0) \propto i s \ln^2 \tilde{s}, \qquad \tilde{s} = -i s/s_0, \quad s_0 = 1 \text{ GeV}^2$$
(8)

lead to

$$\sigma \propto \ln^2(s/s_0). \tag{9}$$

The corresponding maximal behavior of the odd-under-crossing amplitude $A^{(-)}$

$$A^{(-)}(s,t=0) \propto s \ln^2 \tilde{s} \tag{10}$$

leads via the optical theorem, to the difference of the antiparticle-particle and particle-particle total cross sections

$$\Delta\sigma \propto \ln(s/s_0) \tag{11}$$

which grows, in absolute value, with energy. However, the sign of $\Delta \sigma$ is not fixed by general principles.

Such a behaviour (9) is often referred to as "Froissaron", while the behaviour (10) is termed as "Maximal Odderon". At t = 0, they corresponds in the j-plane to a triple pole located at j=1. It was shown in [22] that Froissaron and Maximal Odderon model describes perfectly all the forward scattering TOTEM data [18– 20, including the surprisingly small value of the ratio ρ at $\sqrt{s} = 13$ TeV. Moreover, fit to the data at t = 0of the model with a more general form of FMO [23] shows that one returns to the solution with Froissaron and Maximal Odderon. Extension of the FMO model for $t \neq 0$ was suggested in [24] and leaded to quite good fit in region $\sqrt{s} \geq 5$ at t = 0 and $19 \,\mathrm{GeV} \sqrt{s} \leq 13 \,\mathrm{TeV}$ at $0 < |t| \le 5 \,\text{GeV}^2$. Thus, it would be interesting to consider at least some of the spin effects within this approach.

II. THE MODELS FOR SPIN-NON-FLIP AND SPIN-FLIP AMPLITUDES

As noted above, our aim is study of spin-flip effects, assuming that they are determined mainly by Φ_5 term.

Therefore, we apply to the models considered here the assumption $\Phi_2 = \Phi_3 = \Phi_4 = 0$. If $\Phi_3 \neq 0$ but has the same functional form as Φ_1 then just redefinition of the couplings in Φ_1 can be applied.

A. Simplified FMO model (Model A)

Only the main terms of Froissaron and Maximal Odderon amplitudes in FMO model [24] are taken into account in the model A. At t=0 they correspond to triple poles in j-plane. This truncated crossing-even and crossing-odd terms of FMO model are noted as $P_i^{(T)}(s,t)$ and $O_i^{(T)}(s,t)$.

Thus, in the model A the crossing-even and crossingodd parts of the both spin amplitudes important at high energy are chosen as follows

$$\Phi_i^{(\pm)}(s,t) = P_i(s,t) + R_i^f(s,t) \pm [O_i(s,t) + R_i^{\omega}(s,t)], (12)$$

$$P_i(s,t) = P_i^{(T)}(s,t) + P_i^{(D)}(s,t) + P_i^{(S)}(s,t),$$
 (13)

$$O_i(s,t) = O_i^{(T)}(s,t) + O_i^{(D)}(s,t) + O_i^{(S)}(s,t),$$
 (14)

where i = 1, 5. The full explicit expressions for the model A are given in the Appendix A.

Spin-flip amplitudes are written in the model A in the following form

$$P_5^{(T,D,S,f)}(s,t) = \frac{\sqrt{-t}}{2m} \lambda_+(t) P_1^{(T,D,S,f)}(s,t), \quad (P_i^f \equiv R_i^f),$$
(15)

$$O_5^{(T,D,S,\omega)}(s,t) = \frac{\sqrt{-t}}{2m} \lambda_-(t) O_1^{(T,D,S,\omega)}(s,t), \quad (O_i^{\omega} \equiv R_i^{\omega}).$$
(16)

For $\lambda_{\pm}(t)$ we try in the fit to experimental data three variants

V.1
$$\lambda_{\pm}(t) = 1$$
;

V.2
$$\lambda_{\pm}(t) = 1 + p_{\pm}t;$$

V.3
$$\lambda_{\pm}(t) = 1 + p_{1,\pm}t + p_{2,\pm}t^2$$
.

Matching the model with experimental data are given in the Sect. III.

B. Full FMO model (Model B)

For spin-non-flip amplitudes we use the FMO model at $t \neq 0$ [24]. The only difference of [24] is a notation for constants and functions.

$$\Phi_{i}^{+}(z_{t},t) = P_{i}^{(F)}(z_{t},t) + P_{i}^{(1)}(z_{t},t) + P_{i}^{(2)}(z_{t},t)
+ P_{i}^{(h)}(z_{t},t) + R_{i}^{+}(z_{t},t),
\Phi_{i}^{-}(z_{t},t) = O_{i}^{(M)}(z_{t},t) + O_{i}^{(1)}(z_{t},t) + O_{i}^{(2)}(z_{t},t)
+ O_{i}^{(h)}(z_{t},t) + R_{i}^{-}(z_{t},t).$$
(17)

where $z_t = -1 + 2s/(4m^2 - t) \approx 2s/(4m^2 - t)$ and i = 1, 5.

In the Eq. (17) $P_i^{(F)}, O_i^{(M)}$ are the Froissaron and Maximal Odderon contributions, $P_i^{(1)}, O_i^{(1)}$ are the standard (single j-pole) pomeron and odderon contributions and R_i^+, R_i^- are effective f and ω single j-pole contributions, where j is an angular momentum of these reggeons. $P_i^{(2)}$ and $O_i^{(2)}$ are double PP,OO and PO cuts, correspondingly. We take into account as well the "hard" pomeron and odderon $P_i^{(h)}, O_i^{(h)}$.

We consider the model at $t \neq 0$ and at energy $\sqrt{s} > 19$ GeV, so we neglect the rescatterings of secondary reggeons R_1^+, R_1^- with P and O. In the considered kinematical region they are small. Besides, because f and ω are effective, they can take into account small effects from the cuts via the parameters of them.

The explicit expressions for the spin-non-flip amplitudes in the full FMO model are given in the Appendix B .

We have used for the fit the following forms of spin-flip amplitudes

$$\begin{split} \Phi_5^+(z_t,t) &= \frac{\sqrt{-t}}{2m} \lambda_+(t) \\ &\times \left\{ P_5^{(F)}(z_t,t) + P_5^{(eff)}(z_t,t) + R_5^+(z_t,t) \right\}, \end{split}$$

$$\Phi_{5}^{-}(z_{t},t) = \frac{\sqrt{-t}}{2m} \lambda_{-}(t) \times \left\{ O_{5}^{(M)}(z_{t},t) + O_{5}^{(eff)}(z_{t},t) + R_{5}^{-}(z_{t},t) \right\}.$$
(18)

$$P_{5}^{(F)}(z_{t},t) = h_{5}e^{\beta_{5}(F)\tau_{p}}P_{1}^{(F)}(z_{t},t),$$

$$\tau_{p} = 2m_{\pi} - \sqrt{4m_{\pi}^{2} - t},$$

$$P_{5}^{(eff)}(z_{t},t) = g_{5}^{(P)}e^{\beta_{5}(P)\tau_{p}}P_{1}^{(eff)}(z_{t},t),$$

$$R_{5}^{+}(z_{t},t) = g_{5,+}e^{\beta_{5}^{+}\tau_{p}}R_{1}^{+}(z_{t},t),$$

$$O_{5}^{(M)}(z_{t},t) = o_{5}e^{\beta_{5}(M)\tau_{o}}O_{1}^{(M)}(z_{t},t),$$

$$\tau_{0} = 3m_{\pi} - \sqrt{9m_{\pi}^{2} - t},$$

$$O_{5}^{(eff)}(z_{t},t) = g_{5}^{(O)}e^{\beta_{5}(O)\tau_{o}}O_{1}^{(eff)}(z_{t},t),$$

$$R_{5}^{-}(z_{t},t) = g_{5,-}e^{\beta_{5}^{-}\tau_{o}}R_{1}^{-}(z_{t},t).$$

$$(19)$$

We consider, for the sake of reduced number of free parameters, the sum of all standard pomeron (odderon) terms as one effective pomeron (odderon)

$$P_1^{(eff)}(z_t, t) = P_1^{(1)}(z_t, t) + P_1^{(2)}(z_t, t) + P_1^{(h)}(z_t, t),$$

$$O_1^{(eff)}(z_t, t) = O_1^{(1)}(z_t, t) + O_1^{(2)}(z_t, t) + O_1^{(h)}(z_t, t).$$
(20)

For the functions $\lambda_{+} \pm (t)$ we have explored the same variants as used in the model A (Sect. II A).

III. RESULTS

Free parameters of the models were determined from the fit to the data on $\sigma_{tot}(s)$, $\rho(s,0)$, $d\sigma(s,t)/dt$ and

TABLE I. Data description in the Simplified FMO model (S-FMO) and original FMO model (FMO) with the three choices of the functions $\lambda_{\pm}(t)$ in the spin-fip amplitudes. Comments on number of free parameters in fits are given in Appendix C

			S-F	MO model	$, \chi^2/N$	FM	O model, y	χ^2/N
Process Observable			Variants of $\lambda_{\pm}(t)$ in Eqs. (15), (16)					
			V1	V2	V3	V1	V2	V3
$pp \to pp$	σ_{tot}	110	0.899	0.864	0.865	0.880	0.890	0.894
$\bar{p}p o \bar{p}p$	σ_{tot}	58	2.193	1.271	1.130	0.896	0.900	0.868
$pp \to pp$	ho	67	1.788	1.586	1.587	1.563	1.562	1.564
$\bar{p}p o \bar{p}p$	ho	12	1.267	0.658	0.595	0.389	0,379	0.394
$pp \to pp$	$d\sigma/dt$	1701	1.728	1.630	1.587	1.522	1.513	1.514
$\bar{p}p o \bar{p}p$	$d\sigma/dt$	389	1.359	0.943	0.919	1.106	1.063	1.094
$pp \to pp$	P(t)	49	0.920	1.742	1.483	0.908	0.882	1.105
	n_{par} , number of free parameters		35	37	38	42	44	48
	$\chi^2/NDF = \chi^2/(\sum N_0 - n_{par})$		1.648	1.493	1.449	1.410	1.405	1.405

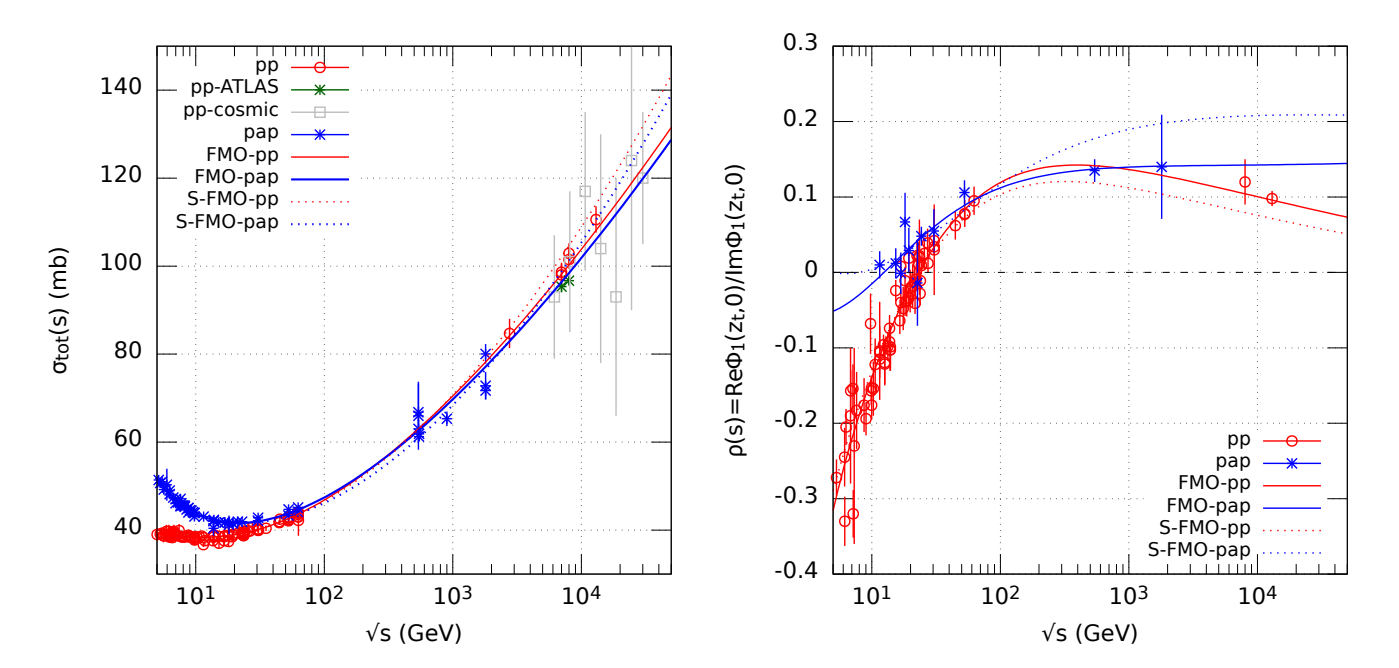


FIG. 1. Total cross sections σ_{tot} and ratio ρ in the variant V1 for models A (dotted line) and B (solid line), $z_t(t=0) = s/2m^2 - 1$

P(t) in the region

$$\begin{array}{lll} \text{for} & \sigma_{tot}(s), \rho(s) & \text{at 5 GeV} \leq \sqrt{s} \leq 13 \text{ TeV}, \\ \text{for} & d\sigma(s,t)/dt & \text{at 19 GeV} \leq \sqrt{s} \leq 13 \text{ TeV}, \\ \text{for} & P_{pp \rightarrow pp}(t) & \text{at } \sqrt{s} = 19.416, \ 23.671 \text{ GeV}. \end{array}$$

The data on σ_{tot} and ρ are taken from the site of Particle Data Group [26]. The recent TOTEM data [17–20] also were added. We did not include to the fit two ATLAS points on σ_{tot} at 7 and 8 TeV (see discussion in [23]). The data on differential cross sections were collected from the big number of the papers from FNAL, ISR, CERN and other experimental collaborations. They

can be found at the Repository for publication-related High-Energy Physics data [27]. Data on polarization included in the data set for fit are taken from the Refs. [8, 9].

Results of the fits in all considered variants of the models A and B are shown in the Table I. Because of the relatively small differences in χ^2 we show the Figurss 1, 2, 3, 4 with theoretical curves for both the models in the simplest variants V1 with $\lambda_{\pm} = 1$. The values and errors of free parameters in the chosen variant V1 are given in the Appendix C in the Tables II and III. One can see from the Figures quite good agreement with the data on cross sections and polarization in kinematic region (21).

quence lower absolute values of the ratio ρ in the simplified FMO model. Additional terms, the "hard" pomeron and odderon (exactly as it is written in the original FMO model) can fix the problem (then χ^2 and curves for σ_{tot} , ρ in both the models almost coincide). We do not discuss here this solution.

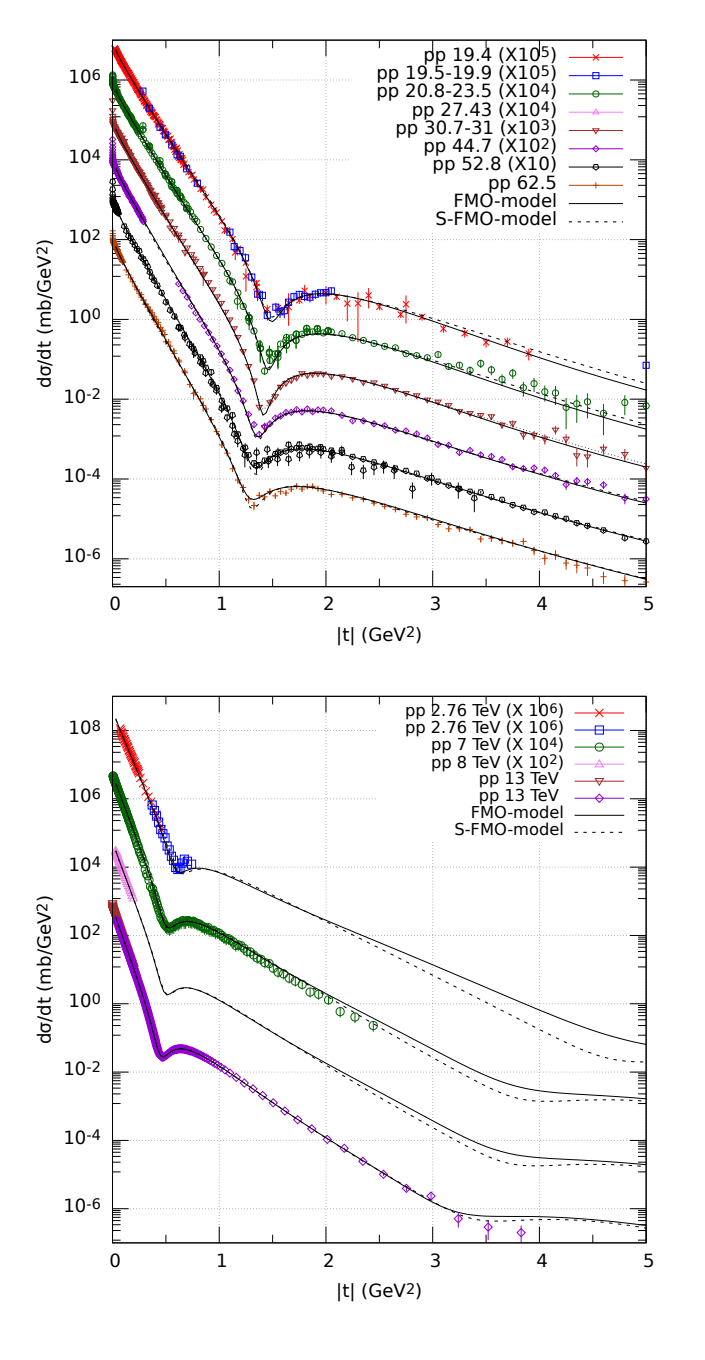


FIG. 2. Differential $pp \to pp$ cross sections at FNAL and ISR energies (upper panel) and at LHC energies (bottom panel)

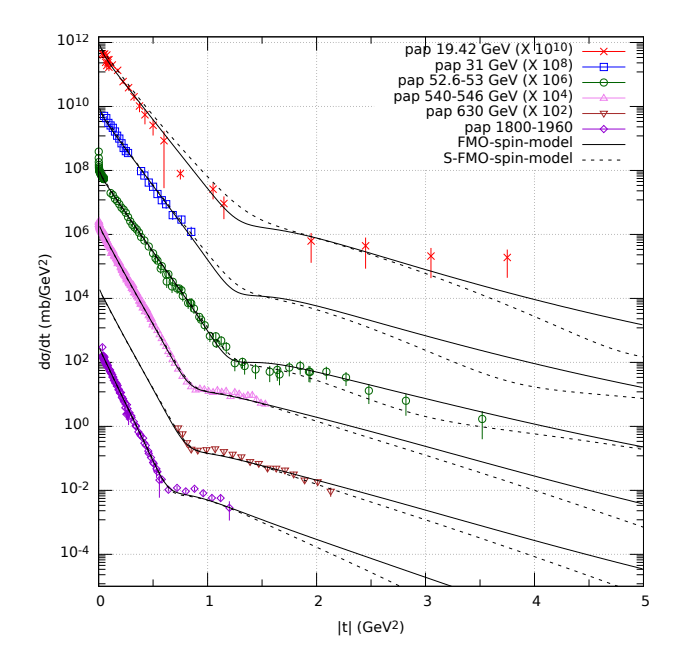


FIG. 3. Differential $\bar{p}p\to\bar{p}p$ cross sections at FNAL, ISR, SPS and Tevatron energies

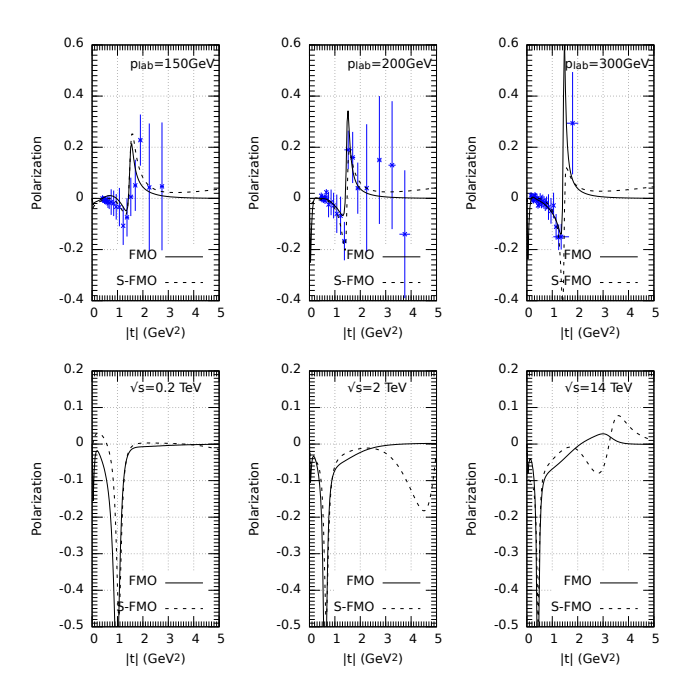


FIG. 4. Polarization at FNAL energies, and extrapolation of P(t) up to \sqrt{s} =13 TeV. Data at p_{lab} =150 GeV did not included in the fit

We confirm conclusions of the Refs. [1, 2, 4, 6, 14] obtained in more traditional pomeron and odderon models that the crossing-even and crossing-odd spin-flip amplitudes are important for agreement with experimental data. It would be not worse to note that polarization in FMO model goes to 0 with rising |t|, while in S-FMO it does not vanish at least at a few GeV².

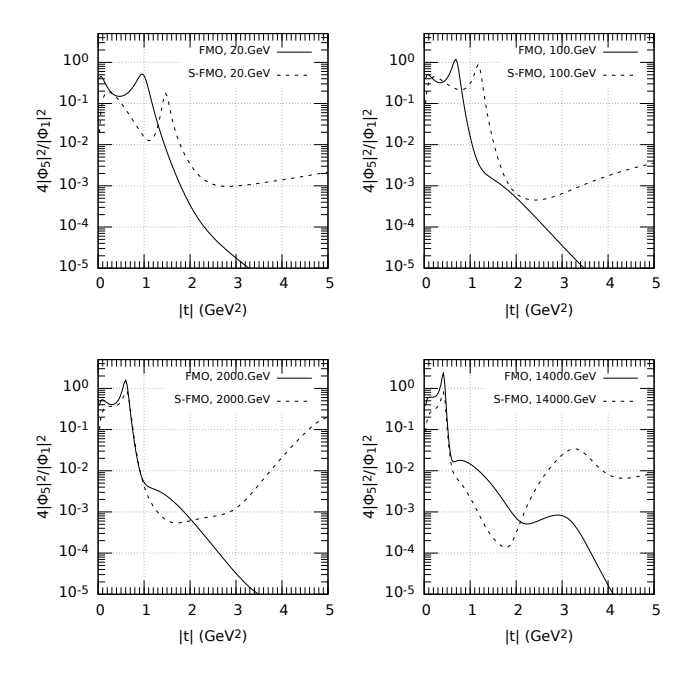


FIG. 5. Ratio $4|\Phi_5|^2/|\Phi_1|^2$ of the contributions to differential pp cross sections

The Fig. 5 demonstrates that the ratios of spin-flip amplitudes to spin-non-flip amplitudes are more important at small and middle |t|, decreasing with increasing |t|. S-MO model predicts more strong spin effects, in particular, in region around dip in the differential cross sections and at higher |t|.

Influence of odderon in the spin-non-flip and spin-flip amplitudes in the considered models one can see in the Fig. 6. Contribution of the Maximal Odderon in non-flip amplitudes at not highest energies is more strong in the original FMO model (red lines) and it is decreasing with |t| slower than in S-FMO model (blue lines). In the "TeV" region situation is opposite. The Maximal Odderon to Froissaron terms ratio in spin-flip components (dashed lines) $(|\Phi^-|_5/|\Phi_5^+| \approx 10\%$ at the $|t| \gtrsim 1-2~{\rm GeV}^2)$ in these models is higher than it was estimated in [2] (\sim 2%).

The last comments in fact give the answers the questions addressed in Introduction about role and magnitude of spin effects in the models within FMO approach.

Thus, concluding the brief discussion of the results we would like to emphasize that considered FMO models taking into account spin-flip effects are in agreement with available experimental data. They predict more important role of spin-flip amplitudes at higher energies and

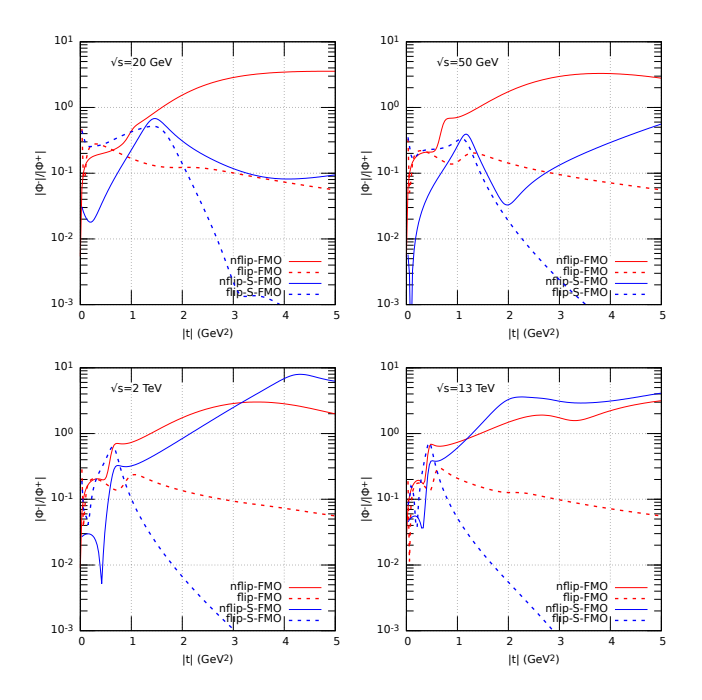


FIG. 6. The ratios of crossing-odd to crossing-even parts of spin-non-flip (solid lines) and spin flip (dashed lines) amplitudes in FMO and S-FMO models

momenta transferred than it is predicted by traditional Regge pole models. Unfortunately, however, there are no data at high energy to confirm or deny these predictions.

Acknowledgment. The authors thank Prof. B. Nicolescu and Prof. S.M. Troshin for a careful reading of the manuscript, comments and useful discussions. E.M. and G.T. were partially supported by the Project of the National Academy of Sciences of Ukraine (0118U003197).

Appendix A: Simplified FMO model

The simple and dipole Pomerons (Odderons) for both components have a conventional form:

$$P_{1}^{(S)}(s,t) = -g_{1,p}^{(S)} \tilde{s}^{\alpha_{p}(t)} e^{\beta_{1,p}^{(S)} \tau_{p}},$$

$$P_{1}^{(D)}(s,t) = -g_{1,p}^{(D)} \xi \tilde{s},^{\alpha_{p}(t)} e^{\beta_{1,p}^{(D)} \tau_{p}},$$

$$\tau_{p} = 2m_{\pi}^{2} - \sqrt{4m_{\pi}^{2} - t}$$
(A1)

$$\begin{split} O_{1}^{(S)}(s,t) &= ig_{1o}^{(S)}\tilde{s}^{\alpha_{o}(t)}e^{\beta_{1,o}^{(S)}\tau_{o}},\\ O_{1}^{(D)}(s,t) &= ig_{1,o}^{(D)}\xi\tilde{s}^{\alpha_{o}(t)}e^{\beta_{1,o}^{(D)}\tau_{0}},\\ \tau_{0} &= 3m_{\pi}^{2} - \sqrt{9m_{\pi}^{2} - t}. \end{split} \tag{A2}$$

where $\tilde{s} = -i(s - 2m^2)/2m^2$, $\xi = \ln(\tilde{s})$.

It is important that we use for single and double jpoles pomeron and odderon intercepts equal to one

$$\alpha_p(t) = 1 + \alpha'_p t, \qquad \alpha_o(t) = 1 + \alpha'_o t.$$
 (A3)

avoiding a violation of unitarity restriction for total cross sections.

$$P_{5}^{(S)}(s,t) = -g_{5,p}^{(S)} \frac{\sqrt{-t}}{2m} \lambda_{+}(t) \tilde{s}^{\alpha_{p}(t)} e^{\beta_{5,p}^{(S)} \tau_{p}},$$

$$P_{5}^{(D)}(s,t) = -g_{5,p}^{(D)} \frac{\sqrt{-t}}{2m} \lambda_{+}(t) \xi \tilde{s}^{\alpha_{p}(t)} e^{\beta_{5,p}^{(D)} \tau_{p}},$$
(A4)

$$\begin{split} O_{5}^{(S)}(s,t) &= ig_{5,o}^{(S)} \frac{\sqrt{-t}}{2m} \lambda_{-}(t) \tilde{s}^{\alpha_{o}(t)} e^{\beta_{1,o}^{(S)} \tau_{o}}, \\ O_{5}^{(D)}(s,t) &= ig_{5,o}^{(D)} \frac{\sqrt{-t}}{2m} \lambda_{-}(t) \xi \tilde{s}^{\alpha_{o}(t)} e^{\beta_{5,o}^{(DS)} \tau_{p}o} \end{split} \tag{A5}$$

where m is proton mass. A choice of $\lambda_{\pm}(t)$ is discussed in the Section II A .

The main tripole terms $P^{(T)}, O^{(T)}$, truncated Froissaron and Maximal Odderon, containing only asymptotic main components from the Froissaron and Maximal Odderon [24]), are selected in according with the AKM asymptotic theorem [25]

$$\begin{split} P_{1}^{(T)}(s,t) &= -g_{1,p}^{(T)}\tilde{s}\xi^{2}\frac{2J_{1}(z_{p})}{z_{p}}e^{\beta_{1,p}^{(T)}\tau_{p}},\\ P_{5}^{(T)}(s,t) &= -g_{5,p}^{(T)}\frac{\sqrt{-t}}{2m}\lambda_{p}(t)\tilde{s}\xi^{2}\frac{2J_{1}(z_{p})}{z_{p}}e^{\beta_{5,p}^{(T)}\tau_{p}}, \end{split} \tag{A6}$$

$$O_{1}^{(T)}(s,t) = ig_{1,o}^{(T)}\tilde{s}\xi^{2} \frac{2J_{1}(z_{o})}{z_{o}} e^{\beta_{1,o}^{(T)}\tau_{o}},$$

$$O_{5}^{(T)}(s,t) = ig_{5,o}^{(T)} \frac{\sqrt{-t}}{2m} \lambda_{o}(t)\tilde{s}\xi^{2} \frac{2J_{1}(z_{o})}{z_{o}} e^{\beta_{1,o}^{(T)}\tau_{o}}$$
(A7)

where $z_p = r_p \tau \xi$, $z_o = r_o \tau \xi$, $\tau = \sqrt{-t/t_0}$, $t_0 = 1 \,\text{GeV}^2$, r_p, r_o are constants.

Contributions of the secondary reggeons, f and ω have a standard form

$$\begin{split} R_{1}^{(f)}(s,t) &= -g_{1}^{(f)} \tilde{s}^{\alpha_{f}(t)} e^{\beta_{1}^{(f)} \tau_{p}}, \\ R_{5}^{(f)}(s,t) &= -g_{5}^{(f)} \frac{\sqrt{-t}}{2m} \lambda_{p}(t) \tilde{s}^{\alpha_{f}(t)} e^{\beta_{5}^{(f)} \tau_{p}}, \\ \alpha_{f}(t) &= \alpha_{f}(0) + \alpha_{f}' t, \end{split} \tag{A8}$$

$$R_1^{(\omega)}(s,t) = ig_1^{(\omega)}\tilde{s}^{\alpha_f(t)}e^{\beta_1^{(\omega)}\tau_o},$$

$$R_5^{(\omega)}(s,t) = ig_5^{(\omega)}\frac{\sqrt{-t}}{2m}\lambda_o(t)\tilde{s}^{\alpha_\omega(t)}e^{\beta_5^{(\omega)}\tau_o},$$

$$\alpha_\omega(t) = \alpha_\omega(0) + \alpha_\omega' t$$
(A9)

Appendix B: Original FMO model

We write here the explicit spin-non-flip terms of FMO model at $t \leq 0$ [24] just for reader's convenience. The only difference of [24] is a notation for constants and

functions. Spin-flip terms are presented and discussed in the Section II B.

Froissaron and Maximal Odderon are written in the following form

$$\begin{split} &\frac{1}{iz}P_{1}^{(F)}(z_{t},t)=h_{1,1}\xi^{2}\frac{2J_{1}(r_{+}\tau\xi)}{r_{+}\tau\xi}e^{\beta_{1,1}^{(F)}\tau_{p}}\\ &+h_{1,2}\xi\frac{\sin(r_{+}\tau\xi)}{r_{+}\tau\xi}e^{\beta_{1,2}^{(F)}\tau_{p}}+h_{1,3}J_{0}(r_{+}\tau\xi)e^{\beta_{1,3}^{(F)}\tau_{p}}, \end{split} \tag{B1}$$

$$\frac{1}{z}O_{1}^{(M)}(z_{t},t) = o_{1,1}\xi^{2} \frac{2J_{1}(r_{-}\tau\xi)}{r_{-}\tau\xi} e^{\beta_{1,1}^{(M)}\tau_{o}}
+o_{1,2}\xi \frac{\sin(r_{-}\tau\xi)}{r_{-}\tau\xi} e^{\beta_{1,2}^{(M)}\tau_{o}} + o_{1,3}J_{0}(r_{-}\tau\xi) e^{\beta_{1,3}^{(M)}\tau_{o}},$$
(B2)

where $z = 2m^2z_t$, $\xi = \ln(-iz_t)$, $\tau = \sqrt{-t/t_0}$, $t_0 = 1 \text{ GeV}^2$, $r_- = r_+ - \delta r_-$, $\delta r_- \ge 0$. It was found in Ref. [24] that the best data description is achieved for minimal allowed $\delta r_- = 0$. This option in the FMO is explored as well in the present paper.

The standard Regge pole contributions have the form

$$R_{1}^{(K)}(z_{t},t) = -\binom{1}{i} 2m^{2} g_{1}^{(K)}(-iz_{t})^{\alpha_{K}(t)}$$

$$\times \left[d_{k} e^{b_{1,1}^{(K)} t} + (1 - d_{k}) e^{b_{1,2}^{(K)} t} \right],$$

$$\alpha_{K}(t) = \alpha_{K}(0) + \alpha'_{K} t,$$

$$K = P, O, f, \omega, \quad k = p, o, \quad d_{\pm} = 1.$$
(B3)

They take into account a possibility of a non pure exponential behaviour of the vertex functions for standard pomeron and odderon [24].

The factor $2m^2$ is inserted in amplitudes $R_1^K(z_t,t)$ in order to have the normalization for amplitudes and dimension of coupling constants (in millibarns) coinciding with those in [22]. The same is made for all other amplitudes.

We have added in FMO as well the double pomeron and odderon cuts, PP,OO,PO in their usual standard form without any new parameters. Namely,

$$P_1^{(2)}(z_t, t) = P_1^{(PP)}(z_t, t) + P_1^{(OO)}(z_t, t),$$

$$O_1^{(2)}(z_t, t) = P_1^{(PO)}(z_t, t),$$
(B4)

$$P_{1}^{(PP)}(z_{t},t) = -i\frac{2m^{2}(z_{t}g_{1}^{(P)})^{2}}{16\pi s\sqrt{1-4m^{2}/s}} \left\{ \frac{d_{p}^{2}}{2B_{1}^{p}} \exp(tB_{1}^{p}/2) + \frac{2d_{p}(1-d_{p})}{B_{1}^{p}+B_{2}^{p}} \exp\left(t\frac{B_{1}^{p}B_{2}^{p}}{B_{1}^{p}+B_{2}^{p}}\right) + \frac{(1-d_{p})^{2}}{2B_{2}^{p}} \exp(tB_{2}^{p}/2) \right\}$$
(B5)

$$P_1^{OO}(z_t, t) = -i \frac{2m^2 (z_t g_1^{(O)})^2}{16\pi s \sqrt{1 - 4m^2/s}} \left\{ \frac{d_o^2}{2B_1^o} \exp(t B_1^o / 2) + \frac{2d_o (1 - d_o)}{B_1^o + B_2^o} \exp\left(t \frac{B_1^o B_2^o}{B_1^o + B_2^o}\right) + \frac{(1 - d_o)^2}{2B_2^o} \exp(t B_2^o / 2) \right\}$$
(B6)

$$P_{1}^{PO}(z_{t},t) = \frac{2m^{2}z_{t}^{2}g_{1}^{(P)}g_{1}^{(O)}}{16\pi s \sqrt{1-4m^{2}/s}} \times \left\{ \frac{d_{p}d_{o}}{B_{1}^{p}+B_{1}^{o}} \exp\left(t\frac{B_{1}^{p}B_{1}^{o}}{B_{1}^{p}+B_{1}^{o}}\right) + \frac{d_{p}(1-d_{o})}{B_{1}^{p}+B_{2}^{o}} \exp\left(t\frac{B_{1}^{p}B_{2}^{o}}{B_{1}^{p}+B_{2}^{o}}\right) + \frac{(1-d_{p})d_{o}}{B_{2}^{p}+B_{1}^{o}} \exp\left(t\frac{B_{2}^{p}B_{1}^{o}}{B_{2}^{p}+B_{1}^{o}}\right) + \frac{(1-d_{p})(1-d_{o})}{B_{2}^{p}+B_{2}^{o}} \exp\left(t\frac{B_{2}^{p}B_{2}^{o}}{B_{2}^{p}+B_{2}^{o}}\right) \right\}$$

where $B_k^{p,o} = b_{1,k}^{P,O} + \alpha'_{P,0} \ln(-iz_t)$, k = 1, 2, $b_{1,k}^{P,O}$ are the constants from single pomeron and odderon contributions.

In [24] it was noted that for a better description of the data it is advisable to add to the amplitudes the contributions that mimic some properties of "hard" pomeron (P^h) and odderon (O^h) . We take them in the simplest form

$$P_1^{(h)}(t) = i2m^2 z_t \frac{g_{h,p}}{(1 - t/t_{p,h})^4},$$

$$O_1^{(h)}(t) = 2m^2 z_t \frac{g_{h,o}}{(1 - t/t_{o,h})^4}.$$
(B8)

Appendix C: Paramters in the models

Number of free parameters is varied in various fits, because we put a reasonable (in our opinion) limits for slopes in exponential vertexes (0 $\leq b, \beta \leq 20\,\mathrm{GeV}^{-1}$) and for trajectories slopes (0.8 $\leq \alpha'_{f,\omega} \leq 1.1\,\mathrm{GeV}^{-2}$). If during fitting such a parameter goes to limit value, then it is fixed at the corresponding limit.

TABLE II: Parameters of the Simplified FMO model (A)

Name	Dimension	Value	Error
$g_{1,p}^{(T)}$	mb	0.29343E+00	0.22854E-03
$\beta_{1,p}^{(T)}$	${ m GeV}^{-1}$	0.51823E+01	0.25651 E-02
r_p		0.29661E+00	0.57101E- 04
α_p'	${ m GeV^{-2}}$	0.16361E+00	0.39431E-03

Continued on next page

TABLE II – Continued from previous page

Name	Dimension	Value	Error
(D)	mb	-0.76106E+00	0.11876E-02
$g_{1,p}^{(D)}$ $\beta_1^{(D)}$	GeV^{-1}	0.19434E+01	0.32444E-02
$a_{\cdot}^{(S)}$	mb	0.27402E+02	0.40164E-01
$g_{1,p}$ $\beta^{(S)}$	GeV^{-1}	0.41323E+01	0.38042E-02
$a^{(T)}$	mb	-0.37472E-01	0.22257E-03
$\beta_{1,o}^{(T)}$	GeV^{-1}	0.33673E+01	0.93166E-02
. 1,0	Gev	0.33073E+01 0.27253E+00	0.93100E-02 0.24894E-03
$r_o \ lpha'_o$	${ m GeV^{-2}}$	0.27255E+00 0.12120E-01	0.45999E-03
$g_{1,o}^{(D)}$			0.45999E-03 0.25831E-02
$g_{1,o}$ $\beta_1^{(D)}$	$^{ m mb}$ ${ m GeV}^{-1}$	0.20536E+00	
$\rho_{1,o}$ (S)		0.65245E+01	0.35911E-01
$g_{1,o}$	mb	0.13783E+01	0.14165E-01
$\beta_{1,o}^{(S)}$	${ m GeV^{-1}}$	0.34116E+01	0.12406E-01
$\alpha_f(0)$	o	0.76576E+00	0.15048E-02
α_f'	${ m GeV^{-2}}$	0.80000E+00	fixed at limit
$g_1^{(f)}$	mb	0.35167E+02	0.24485E+00
$\beta_1^{(f)}$	${ m GeV^{-1}}$	0.00000E+00	fixed at limit
$\alpha_{\omega}(0)$		0.61636E+00	0.58521E-02
α_{ω}'	${ m GeV^{-2}}$	0.80000E+00	fixed at limit
$g_1^{(\omega)}$	mb	$0.24366\mathrm{E}{+02}$	0.35434E+00
$\beta_1^{(\omega)}$	${ m GeV^{-1}}$	$0.20000\mathrm{E}{+02}$	fixed at limi
$g_{5,p}^{(T)}$	mb	$0.98237\mathrm{E}{+00}$	0.29269 E-02
$\beta_{5,p}^{(T)}$	${ m GeV^{-1}}$	0.97449E + 01	0.11045 E-01
$g_{5,p}^{(D)}$	mb	-0.23787E + 02	0.71732 E-01
$\beta_{5,p}^{(D)}$	${ m GeV^{-1}}$	0.12183E+02	0.11698E- 01
$g_{5,p}^{(S)}$	mb	0.29036E+03	0.70315E+00
$\beta_{5,p}^{(S)}$	${\rm GeV}^{-1}$	0.97486E+01	0.80005E- 02
$g_{5,o}^{(T)}$	${ m mb}$	0.57721E- 03	0.57266E- 03
$\beta_{5,0}^{(T)}$	${\rm GeV^{-1}}$	0.26306E+01	0.96362E+00
$g_{5,0}^{(D)}$	mb	0.77319E+01	0.13988E+00
$\beta_{5,a}^{(D)}$	${\rm GeV}^{-1}$	0.14185E+02	0.63904E-01
$a_{\mathbf{z}}^{(S)}$	mb	-0.69382E+02	0.14333E+01
$\beta_{5,o}^{(S)}$	GeV^{-1}	0.12588E+02	•
$g_5^{(f)}$	mb	-0.58675E+03	
$\beta_{\varepsilon}^{(f)}$	GeV^{-1}	0.92251E+01	·
$a_{\epsilon}^{(\omega)}$	mb	0.29637E+02	
$\beta_5^{(\omega)}$	GeV^{-1}	0.00000E+00	•
~ 5	J	5.500002,00	

TABLE III: Parameters of the FMO model (B)

Name	Dimension	Value	Error
$h_{1,1}$	${ m mb}$	0.14330E+00	0.11569 E-03
$h_{1,2}$	${ m mb}$	0.29852E+01	0.54259 E-02
$h_{1,3}$	${ m mb}$	0.90696E+01	0.10925E+00
r_{+}		0.26288E+00	0.54777E-04
$\beta_{1,1}^{(F)}$	${\rm GeV}^{-1}$	0.23291E+01	0.13574 E-02

 $Continued\ on\ next\ page$

TABLE III - Continued from previous page

Name	Dimension	Value	Error
$\beta_{1,2}^{(F)}$	${ m GeV^{-1}}$	0.39343E+01	0.44429E-02
$\beta_{1,3}^{(F)}$	${ m GeV^{-1}}$	0.15649E + 02	0.67054E+00
$o_{1,1}$	${ m mb}$	-0.42452E-01	0.16579 E-03
$o_{1,2}$	${ m mb}$	$0.94686\mathrm{E}{+00}$	0.17991E- 01
$o_{1,3}$	${ m mb}$	$\text{-}0.14200\mathrm{E}{+02}$	0.10239E+00
r_{-}		$0.26288\mathrm{E}{+00}$	fixed: $r = r_+$
$\beta_{1,1}^{(O)}$	GeV^{-1}	0.15717E + 01	0.34223 E-02
$\beta_{1,2}^{(O)}$	${ m GeV^{-1}}$	0.56167E + 01	0.14887E + 00
$\beta_{1,3}^{(O)}$	${ m GeV^{-1}}$	0.31265E+01	0.93369 E-02
α_p'	${ m GeV^{-2}}$	$0.17820\mathrm{E}{+00}$	0.15904 E-03
$g_1^{(P)}$	${ m mb}$	$0.71055\mathrm{E}{+02}$	0.56702 E-01
d_p	${ m mb}$	$0.73915\mathrm{E}{+00}$	0.74388E- 03
$b_{1,1}^{(P)}$	${ m GeV^{-2}}$	$0.52382\mathrm{E}{+01}$	0.49458 E-02
$b_{1,2}^{(P)}$	${ m GeV^{-2}}$	0.21387E + 01	0.29922 E-02
α_o'	GeV^{-2}	0.41252 E-02	0.15522 E-03
$g_1^{(Od)}$	${ m mb}$	$0.27241\mathrm{E}{+02}$	0.36231 E-01
d_o	${ m mb}$	$0.75363\mathrm{E}{+00}$	0.70380 E-03
$b_{1,1}^{(Od)}$	${ m GeV^{-2}}$	0.62168E+01	0.88381E- 02
$b_{1,2}^{(Od)}$	${\rm GeV}^{-2}$	0.21600E + 01	0.26952 E-02
$\alpha_f(0)$		0.76841E+00	0.10061 E-02
$lpha_f'$	${ m GeV^{-2}}$	0.11000E+01	fixed at limit

$g_1^{(f)}$	mb	0.70300E + 02	$0.24332\mathrm{E}{+00}$
$b_{1,f}$	${ m GeV^{-2}}$	0.11101E + 02	0.28189E + 00
$\alpha_{\omega}(0)$		0.31275E+00	0.11785E- 01
$lpha_\omega'$	${ m GeV^{-1}}$	0.11000E+01	fixed at limit
$g_1^{(\omega)}$	mb	0.34042E+02	0.11844E+01
$b_{1,\omega}$	${ m GeV^{-2}}$	0.14447E+01	0.22569E+00
$g_{p,h}$	mb	-0.73998E+02	0.45714 E-01
$t_{p,h}$	${ m GeV^2}$	0.38841E+00	0.14919E- 03
$g_{o,h}$	mb	0.32403E+02	0.42717 E-01
$t_{o,h}$	${ m GeV^2}$	0.61854E+00	0.51543E- 03
h_5	mb	0.38020E+01	0.53841E- 02
$\beta_5^{(F)}$	${ m GeV^{-1}}$	0.31399E+01	0.49814 E-02
O_5	mb	0.38312E+01	0.15409E+00
$\beta_5^{(O)}$	${ m GeV^{-1}}$	0.66434E+01	0.13773E+00
$g_{5,p}$	mb	0.28732E + 01	0.34589E + 00
$\beta_{5,p}$	${ m GeV^{-1}}$	0.13172E+02	0.69818E+00
$g_{5,o}$	mb	0.18954E+02	0.16931E + 01
$\beta_{5,o}$	${ m GeV^{-1}}$	0.20000E+02	fixed at limit
$g_{5,f}$	mb	0.29711E+01	0.17843E+00
$\beta_{5,f}$	${ m GeV^{-1}}$	0.00000E+00	fixed at limit
$g_{5,\omega}$	mb	-0.15919E+02	0.13466E + 01
$\beta_{5,\omega}$	${ m GeV^{-1}}$	0.00000E+00	fixed at limit

- N.H. Buttimore et al. Phys.Rev. The spin dependence of high-energy proton scattering. D59 (1999) 114010; https://arxiv.org/abs/hep-ph/9901339v1
- [2] E. Leader, Spin in Particle Physics, Cambridge University Press, 2001, 500 pp.
- [3] C. Ewerz, P. Lebiedowicz, O. Nachtmann, A. Szczurek, Physics Letters B 763 (2016) 382; https://arxiv.org/abs/1606.08067v1.
- [4] S.Donnachie, G. Dosch, P. Landshoff, O. Nachtmann. Pomeron Physics and QCD, Cambridge University Press. 2002.
- [5] S.M. Troshin, N.E. Tyurin, World Scientific Publishing Company (October 1, 1994).
- [6] A.F. Martini, E. Predazzi, Diffractive effects in spin flip pp amplitudes and predictions for relativistic energies, Phys.Rev.D 66 (2002) 034029; https://arxiv.org/abs/hep-ph/0209027v1; K. Hinotani, H.A. Neal, E. Predazzi and G.Walters. Behavior of the Spin-Flip Amplitude in High-Energy Proton-Proton and Pion-Proton Elastic Scatterings, Nuovo Cimento 52 A (1979) 363.
- [7] G.Fidecaro et al. Measurement of the polarization parameter in pp elastic scattering at p_{lab} =150 GeV/c. Nucl. Phys. B173 (1980) 513.
- [8] G.Fidecaro et al. Measurement of the differential cross section and of the polarization parameter in pp elastic scattering at p_{lab} =200 GeV/c. Phys.Lett. 105B (1981)309.

- [9] R.V.Kline et al. Polarization parameters and angular distributions in pi-p elastic scattering at 100 GeV/c and in pp elastic scattering at $p_{lab}100$ GeV/c and 300 GeV/c. Phys.Rev. D 22 (1980) 553.
- [10] L. Adamczyk et al., STAR Collaboration, Single spin asymmetry A_N in polarized proton–proton elastic scattering at \sqrt{s} = 200 GeV, Physics Letters B 719 (2013) 62–69; https://arxiv.org/abs/1206.1928v3.
- [11] K.G.Boreskov, A.M.Lapidus, S.T.Sukhorukov, K.A.Ter-Martirosyan. Elastic scattering and charge exchange reactions at high energy in the theory of complex angular momentum. Sov. J. Nucl. Phys. 14 (1971) 814.
- [12] J.-R. Cudell, E. Predazzi and O.V. Selyugin. High-energy hadron spin-flip amplitude at small momentum transfer and new A_{ν} data from RHIC. EPJ A (2004) 10012-2; https://arxiv.org/abs/hep-ph/0401040v1.
- [13] B. Z. Kopeliovich, M. Krelina, Probing the Pomeron spin-flip with Coulomb-nuclear interference, https://arxiv.org/abs/1910.04799v3.
- [14] O.V. Selyugin, J.R. Cudell, Odderon, HEGS model and LHC data, Acta Phys. Polon. Supp. 12 (2019) 4; https://arxiv.org/abs/1810.11538v1.
- [15] O.V.Selyugin, High Energy Hadron Spin Flip Amplitude, Phys. Part. Nucl. Lett. 13 (2016) 3, 303; https://arxiv.org/abs/1512.05130v1.
- [16] M.V. Galynskii, E.A.Kuraev. Alternative way to understand the unexpected result of JLab polarization, Phys.Rev. D 89 (2014) 054005; https://arxiv.org/abs/1312.3742v3.

- [17] TOTEM Collaboration, G. Antchev et al. Proton-proton elastic scattering at the LHC energy of \sqrt{s} =7 TeV. EPL 95 (2011) 41001: https://arxiv.org/abs/1110.1385v1; First measurement of the total proton-proton cross-section at the LHC energy of \sqrt{s} = 7 TeV. EPL 96 (2011) 21002; https://arxiv.org/abs/1110.1395v1; Measurement of proton-proton elastic scattering and total cross-section at \sqrt{s} = 7 TeV. EPL 101 (2013) 21002; CERN-PH-EP-2012-352.pdf; Luminosity-independent measurements of total, elastic and inelastic cross-section at \sqrt{s} = 7 TeV, EPL 101 (2013) 21004; CERN-PH-EP-2012-353.pdf.
- [18] TOTEM Collaboration, G. Antchev et al. Luminosity-independent measurements of proton-proton total cross section at $\sqrt{s}=8$ TeV Phys. Rev. Lett. 111, 012001 (2013); CERN-PH-EP-2012-354; Evidence for Non-Exponential elastic proton-proton differential cross section at low |t| and $\sqrt{s}=8$ TeV, Nucl. Phys. B899 (2015) 527; https://arxiv.org/abs/1503.08111v4; Measurement of elastic pp scattering at $\sqrt{s}=8$ TeV in the Coulomb—Nuclear interference region—determination of the ρ parameter and the total cross section. Eur.Phys.J. C76 (2016) 661; https://arxiv.org/abs/1610.00603v1.
- [19] TOTEM Collaboration, G. Antchev et al. First measurement of elastic, inelastic and total cross section at \sqrt{s} =13 TeV by TOTEM and overview of cross section data at LHC energies. Eur. Phys. J. C 79 (2019) 103; https://arxiv.org/abs/1712.06153v2; First determination of the ρ parameter at \sqrt{s} =13 TeV: probing the existence of a colourless C-odd

- three-gluon compound state, Eur. Phys. J. C 79 (2019) 785; https://arxiv.org/abs/1812.04732v1; Elastic differential cross-section measurement at \sqrt{s} =13 TeV by TOTEM. Eur.Phys.J. C 79 (2019) 861; https://arxiv.org/abs/1812.08283v1.
- [20] TOTEM Collaboration, G. Antchev et al. Elastic differential cross-section at $\sqrt{s}=2.76$ TeV and implications on the existence of a colorless 3-gluon bound state. Eur.Phys.J. C80 (2020) 91; https://arxiv.org/abs/1812.08610v1.
- [21] L. Lukazsuk, B. Nicolescu, Lett. Nuovo Cim. 8 (1973) 405.
- [22] E. Martynov, B. Nicolescu. Did TOTEM experiment discover the Odderon? Phys.Lett. B778, 414(2018); https://arxiv.org/abs/1711.03288v6.
- [23] E. Martynov, B. Nicolescu. Evidence for maximality of strong interactions from LHC forward data, B786 (2018) 207; https://arxiv.org/abs/1804.10139v3.
- [24] E. Martynov, B. Nicolescu. Odderon effects in the differential cross-sections at Tevatron and LHC energies. EPJ C, 79, 461 (2019); https://arxiv.org/abs/1808.08580v3
- [25] G. Auberson, T. Kinoshita, and A. Martin, Phys. Rev. D, 3, 3185 (1971).
- [26] https://pdg.lbl.gov/2017; C. Patrignani et al. (Particle Data Group), Chin. Phys. C, 40, 100001 (2016) and 2017 update;
 - https://pdg.lbl.gov/2017/hadronic-xsections/hadron.html
- [27] https://www.hepdata.net (the old version of the Data Base is available at http://hepdata.cedar.ac.uk).